UPLC-ESI-MS/MS strategy to analyze fatty acids composition and lipid profiles of Pacific saury (*Cololabis saira*)

Xinyi Tao [a], Mingyu Yin [a], Liu Lin [a], Rongzhen Song [b], Xiaodong Wang [c], Ningping Tao [a,*], Xichang Wang [a]

[a] *College of Food Science and Technology, Shanghai Ocean University, Shanghai 201306, China*
[b] *College of Food Science and Pharmaceutical Engineering Zaozhuang University, 277160, China*
[c] *College of Fisheries and Life Science, Shanghai Ocean University, Shanghai 201306, China*

ARTICLE INFO

ABSTRACT

The Pacific saury (*Cololabis saira*) is a highly nutritious deep-sea fish, rich in omega-3 polyunsaturated fatty acids (n-3 PUFAs). This study comprehensively investigated fatty acids composition and lipid profiles of different parts of Pacific saury based on an untargeted lipidomic strategy. Results suggested that the crude fat content of meat, head and viscera were 5.81%, 10.90%, and 19.46%, respectively. The contents of PUFAs were 41.08%, 34.96% and 33.14%, respectively. Among them, the n-3 PUFAs in the head (34.58%) were significantly higher than meat (29.40%) and viscera (27.95%). Moreover, 5752 lipid molecules were identified, where glycerophospholipids (GP) were the most numerous lipid type (45.58%), with phosphatidylcholine (PC) being main differential sub-class. PC (20:3_22:6) was the most abundant molecule in the head (14.59%) and meat (19.60%). Head_vs_viscera group had higher characteristic PC abundance. This study will provide a theoretical basis for the physiological activity and lipid high-value utilization of Pacific saury.

1. Introduction

Lipids have been acknowledged as one of the macro-nutrients and exert many exclusive biological activities. Apart from providing energy, they are also an important part of the membrane of the organism and a precursor substance for signaling micro-molecules. Lipids would be involved in the body metabolism, growth and development, neural signaling and other physiological processes (Song et al., 2022). It is categorized into the following eight groups based on their structure and synthetic pathways: fatty acyls (FA), glycerolipids (GL), glycerophospholipids (GP), sphingolipids (SP), sterol lipids (ST), prenol lipids (PreL), saccharolipids (SL) and polyketides (PK) (Behrouz & Yari, 2022). Among them, phospholipids due to their unique amphiphilic structural features, enable lipid micellar solubilization in the tubular lumen, thus promoting lipid hydrolysis and absorption in intestinal epithelial cells, which is significant in intracellular transport and metabolic effects of lipid molecules (Lordan et al., 2017). Therefore, supplementation of phospholipids could repair damaged cell membranes, improve membrane fluidity and membrane enzyme activity, add membrane fatty acid

unsaturation (Nisticò et al., 2023), thus improving antioxidant and anti-aging properties, which increases the protective effects on vascular protection and permeability maintenance (Assmann et al., 2018; Dowhan, 2017).

Compared with soy and egg sources, marine phospholipids are rich in omega-3 polyunsaturated fatty acids (n-3 PUFAs), especially docosahexaenoic acid (DHA) and eicosapentaenoic acid (EPA) (Valencia-Naranjo et al., 2022). The Pacific saury (*Cololabis saira*) is a surface-migratory fish found in the junction of cold and warm currents, and is widely distributed in the subtropical and temperate waters of the Pacific Ocean along the coasts of Asia and American (Wang, 2023). Owing to its delicious taste and high nutritional value, this fish has gradually been popular among consumers. The lipid analysis of Pacific saury study showed that, 9 polyunsaturated fatty acids (PUFAs) accounted for 47.23%–49.66% in total FAs, n-3 PUFAs were predominant. ALA and DHA + EPA accounted for 15.44%–20.67% and 24.85%–27.56%, respectively (Wang, Kong, et al., 2022). n-3 PUFAs could be found in nature either in triglyceride (TG) or phospholipid (PL) form. From brain health view, PL n-3 is more bioavailable and potent compared to TG n-3,

---

as only PL n-3 is able to cross the blood-brain barrier and be involved in brain biochemical reactions (Haq et al., 2021). In addition, marine-derived phospholipids have other physiological activities, such as regulating lipoprotein metabolism (Ahmmed et al., 2020), reducing cholesterol levels (Das, 2018), protecting liver function (Manual Kollareth et al., 2020), lowering inflammatory response and regulating intestinal flora (Ong et al., 2021). Phosphatidylcholine (PC) is the most abundant PL and the most dominant PL molecular species. It's been proven that PC could slow down the aging level of organs, repair the skin aging damage (Wang, Zhao, et al., 2022), regulate the intestinal barrier function, remodel the structure of intestinal flora, and reduce the inflammatory response (Nandi et al., 2021).

The current separation methods for phospholipids mainly include thin-layer chromatography (TLC), high-performance liquid chromatography (HPLC), gas chromatography (GC), nuclear magnetic resonance spectroscopy (NMR) and mass spectrometry (MS). Lipidomic analysis could efficiently study the changes and functions of lipid families and lipid molecules in various biological processes, and elucidate the related biological activities and mechanisms. GC is a powerful analytical technique for separating, identifying and quantifying individual chemical components in complex mixtures, so it has been the most widely used method for the determination of fatty acids in samples (Ahmmed et al., 2021; Ochiai & Komiya, 2021; Petenuci et al., 2021). Liquid chromatography (LC) has been used in the detection of phospholipids, which is capable of rapid separation and quantitative analysis of various phospholipids due to its high separation efficiency, high detection sensitivity and good selectivity (Tam et al., 2018). Electrospray ionization tandem-mass spectrometry (ESI-MS) is one of the most widely used mass spectrometry methods, which has the advantages of high resolution, high detection sensitivity and high selectivity, and is capable of rapid qualitative and quantitative analysis of phospholipids (Cui et al., 2021; Yaghmour et al., 2021; Zhang, Guo, et al., 2022). Therefore, MS combined with LC and allows quantitative detection of lipids in complex lipid mixtures through its unique mass properties (Ferraris et al., 2022; Li et al., 2018; Sun et al., 2022). Liquid chromatography-mass spectrometry (LC-MS) is commonly used for lipidomic analysis, including marine aquatic products such as capelin (*Mallotus villosus*) (Yin et al., 2024), Pacific white shrimp (*Litopenaeus vannamei*) (Duan et al., 2022), shrimp head, codfish roe, and squid gonad (Li et al., 2018), as well as oil crops such as peanuts (Zhang, Guo, et al., 2022) and walnuts (Wang, Zhong, et al., 2022), and hazelnut oil (Sun et al., 2022).

In this study, Pacific saury was divided into head, meat and viscera. GC and ultra-performance liquid chromatography-electrospray ionization tandem mass spectrometry (UPLC-ESI-MS/MS) were applied to determine and compare the basic nutrient composition, physicochemical properties, fatty acids composition and lipid profiles among different parts of Pacific saury. The results are expected to provide ideas for its high-value utilization and the development of marine-derived phospholipids.

2. Materials and methods

2.1. Materials and reagents

The frozen Pacific saury (*Cololabis saira*, 118.29 ± 8.31 g, 30.87 ± 0.79 cm, *n* = 203) was caught in the North Pacific Ocean in October 2023. Subsequently, the samples were transported to the laboratory via a cold chain. After thawing at 4 °C, the samples were dissected into head, meat, viscera. The tissue index of the head, meat and viscera were accounted for 14.04 ± 1.22%, 68.04 ± 7.30%, 7.16 ± 1.07%, respectively. The samples were separately packed in opaque polyethylene bags (50 g per bag) and stored in −80 °C for further analysis.

2.2. Proximate chemical analysis

The samples were analyzed for the proximate composition according

to the Association of Official Analytical Chemists (AOAC, 2019): AOAC 925.40 for moisture content, AOAC 923.03 for ash content, AOAC 920.152 for crude protein content, and AOAC 2003.05 for crude fat.

2.3. Extraction of total lipid

The total lipids were extracted with reference to the Folch method (Song et al., 2022). Head, meat and viscera portioned sample were taken and dried continuously for 72 h in a vacuum freeze dryer (FD-1C-50, Bo Medical Kang Experimental Instrument Co, China.). Briefly, samples (lyophilized powders) were first weighed 30.0 g accurately, 450 mL of chloroform-methanol solution (2,1, v: v) was add and place in the refrigerator at 4 °C for 24 h. The solution was filtered to remove insoluble impurities, 9% NaCl solution (20% of total volume) was added and mixed well, then continue to place at 4 °C for 4 h, waiting for stratification. The upper aqueous layer was removed, and 9% NaCl solution (10% of total volume) was added and mixed for about 2 h, and the upper aqueous layer was removed again. The obtained solution was filtered through anhydrous sodium sulfate and dried by vacuum spinning at 40 °C to obtain the total lipid.

2.4. Physicochemical indicators

The samples were analyzed for chemical composition according to the American Association of Analytical Chemists AOAC (AOAC, 2019); AOAC 969.17 Acid Price, AOAC 993.20 Iodine Value, and AOAC 965.33 Peroxide Value.

2.5. Fatty acids composition

The fatty acids (FAs) composition was carried out with reference to previous studies (Zhang et al., 2019). Accurately weigh 0.1 g (0.001 g) of the extracted total lipids and add 5 mL of 0.5 M NaOH-CH_3OH and 100 μL of 10 mg/mL nonadecanoic acid (C19:0) and mix well and then shaking at 100 °C for 10 min; add 3 mL of 14% BF_3- CH_3OH and shaking for 5 min at 100 °C; add 3 mL of n-hexane and shaking for 2 min at 100 °C; add 2 mL of n-hexane and shaking for 2 min at 100 °C. After that, quickly add 10 mL of saturated NaCl solution to the reacted system, fully shaken, to let stand and layering, then extract the upper layer of the clarified organic phase layer, later filtered with 0.22 μm organic phase filter membrane in the injection bottle, and finally analyzed by GC.

The GC setup was equipped with an Agilent (Santa Clara, CA, USA) SP-2560 capillary column (100 m × 250 μm × 0.2 μm) and a flame ionization detector (Thermo Fisher Scientific, Waltham, MA, USA). The heating procedure was 70 °C at the beginning, and the temperature was increased to 140 °C (50 °C/min) for 1 min, then increased to 180 °C (4 °C/min) for 1 min, then increased to 225 °C (3 °C/min) for 30 min. The temperature of the inlet port was 260 °C, and the injection volume was 1 μL, the split ratio was 45:1. The injection volume was 1 μL, the flow rate was 45:1, the column flow rate was 1 mL/min, and the carrier gas was nitrogen. External standard 37 fatty acid standards and internal standard C19:0 was used to analyzed the fatty acid content in different samples.

2.6. QC samples and sample pre-handling

Aliquots of each group of samples were mixed to form QC. QC samples were not only used to determine the state of the instrument and the equilibrium of the chromatography-mass spectrometry system prior to injection, but also were interspersed with the samples to be tested to evaluate the stability of the system throughout the entire experimental process.

The samples were taken in appropriate quantities, first add 100–200 μL of ultrapure water, vortex for 30 s mix well; then add 800 μL of MTBE, vortex again for 30 s; add 200–240 μL of pre-cooled isopropanol, vortex for 30 s, sonicate for 15–20 min in a water bath at 4 °C, and then leave it

at room temperature for 45 min, and then centrifuge at 12000 rpm for 20 min at 8 °C, take the upper organic phase and blow dry with N_2. Three parallel samples were prepared for each sample.

For mass spectrometry, 150–200 μL of 95% isopropanol-acetonitrile solution was added to dissolve the sample again, and then vortexed for 45 s. 85 μL of the sample was dissolved again, and then centrifuged at 12000 rpm 8 °C for 20 min, and then the upper layer of the sample was taken from centrifugation tubes for chromatographic analysis.

2.7. Chromatographic conditions

The separation was performed on an UHPLC Nexera LC-30 A ultra-high performance liquid chromatography (UHPLC) system (SHI-MADZU, Japan) coupled to Q-Exactive Plus (Thermo Scientific in Shanghai Applied Protein Technology Co., Ltd.) and using ACQUITY UPLC CSH C_{18} Column (1.7 μm, 2.1 mm × 100 mm, Waters) at 45 °C with a flow rate of 300 μL/min. The mobile phase A was composed of acetonitrile aqueous solution (6:4, v: v) with 0.1% formic acid and 0.1 Mm ammonium formate; mobile phase B was composed of acetonitrile isopropanol solution (1:9, v: v) with 0.1% formic acid and 0.1 Mm ammonium formate. The procedure using gradient elution was as follows: mobile phase B was maintained at 30% during 0–2 min; mobile phase B linearly increased to 100% during 2–25 min; and mobile phase B was maintained at 30% during 25–35 min. During the separation process of liquid chromatography, the samples were always placed in a 10 °C autosampler. To avoid the effects caused by fluctuations in the detection signal of the instrument, a randomized sequence was used for continuous analysis of the samples.

2.8. Mass spectrometry conditions

Electrospray ionization (ESI) was used to detect positive and negative ions. The samples were separated by UHPLC and analyzed by a Q-exactive mass spectrometer. The ESI source conditions are as follows: heater temperature 300 °C, sheath gas flow rate 45 arb, aux gas flow rate 15 arb, sweep gas flow rate 1 arb, spray voltage 3.0 KV, capillary temperature 350 °C, S-Lens RF level 50%, MS1 scan ranges: 200–1800. The mass charge ratio of lipid molecules and lipid fragments was collected according to the following methods: 10 fragments (MS2scan, HCD) were collected after each full scan. The resolution of MS1 is 70,000 at m/z 200 and that of MS2 is 17,500 at m/z 200.

Lipidsearch (Thermo Fisher Scientific, USA) was used to extract and identify the peaks of lipid molecules and internal standard lipid molecules. The main parameters were as follows: precursor tolerance: 5 ppm, product tolerance: 5 ppm, product ion threshold:5%.

2.9. Data processing

All the scientific data collected were subjected to three parallel determinations and the results of the collection were expressed as mean ± S.D. SPSS 16.0 was used to analyze the collected scientific data for analysis of variance (ANOVA) and Duncan's method was used to analyze the significance. Scientific data mapping was plotted using Origin 2018. Multivariate statistical analyses including: principal component analysis (PCA), orthogonal partial least squares-discriminant analysis (OPLS-DA) were plotted by SIMCA. Volcano plots and Venn plots were plotted via GraphPadPrism 9. Correlation heat map was plotted by TBtools (Toolbox for Biologists v1. 098745). Neural network maps were plotted through cytoscape_v3.10.0. Fish oil sample VIP values (Variable importance in projection) were generated by OPLS-DA.

3. Results and discussion

3.1. Approximate composition

Basic nutrient content is one of the fundamental indicators for

evaluating the composition of aquatic products, which includes moisture, crude protein, crude fat and ash. Among them, the moisture of the head (68.36 ± 1.49%) was significantly higher than that of viscera (60.04 ± 2.36%) and meat (58.55 ± 1.14%) ($p < 0.05$) (Fig. 1A). The moisture of aquatic products ranges from about 50% to 80%, which can be affected by season, feed, spawning condition, fish body parts and age (Bledsoe et al., 2003). The moisture content of Pacific saury heads was similar to that of tuna heads (67.24 ± 1.87%) (Wang et al., 2021) and salmon head (70.69 ± 2.89%) (Chen et al., 2022), lower than bighead carp head (80.79 ± 1.07%) (Su et al., 2019)and capelin head (81.58 ± 1.37%)(Yin et al., 2022), higher than king salmon head (49.02 ± 1.10%) (Ahmmed et al., 2021).The crude protein content of Pacific saury body meat (20.58 ± 0.03%) was significantly higher than that of the head (15.51 ± 0.82%) and viscera (11.01 ± 0.29%) (p < 0.05). YE et al. studied the nutrient composition of Pacific saury meat, which had a crude protein content of about 17.63 ± 0.34% (Ye et al., 2013). The crude fat content of the viscera (20.46 ± 0.30%) was significantly higher than that of the body meat (10.90 ± 0.35%) and the head (2.81 ± 0.04%) (p < 0.05). These results were lower than bluefin tuna (19.34–30.29%) (Liu et al., 2023), much higher than *tamagoyaki* (4.13% to 6.09%) (Liu, Wang, et al., 2022), sea lamprey (2.00% to 6.08%) (Zeng et al., 2002) and small yellowtail (1.78% to 3.25%) (Gao et al., 2020). Because Pacific saury is a deep-sea fish that lives in temperate or subtropical waters, it is sensitive to temperature changes and is a surface migratory fish, and therefore stores a large amount of fat in its body (Wang, 2023). The ash content in the head of Pacific saury is significantly higher than that in the body meat and viscera, probably because the head covers the skeletal structure of the gill cover, the end of the muzzle, the upper and lower jaws, and the small fins, and thus the head of Pacific saury is rich in minerals, especially calcium. In summary, Pacific saury is a kind of high-protein and medium-fat source, with a high fat content in the viscera, a high protein content in the meat, and a high mineral content in the head.

Acid value (AV) is used to measure the number of free groups in fats and oils, the more carboxylic acid groups reflect the more free FAs in fats and oils, the greater the degree of oxidation. Iodine value (IV) is applied to express the degree of unsaturation of the fats and oils. Peroxide value (POV) is referred to as the amount of primary lipid oxidation products in the process of lipid oxidation, and it is one of the important indicators for evaluating the quality of fats and oils (Fang et al., 2022). The physicochemical indexes of crude fish oil from different parts of saury were demonstrated in Fig. 1B-D. The results of AV showed that: meat < head < viscera, which all below 15 mg/g, indicating that free fatty acids were in the moderate range. The IV showed that: meat > viscera > head, and the data were all above 120 g/100 g, which proved that the degree of unsaturation in fish oil was high and rich in polyunsaturated fatty acids. The POV showed that: meat<head<viscera, all of them were much lower than the CODEX standards for physicochemical properties of fish oils ($\leq$ 2.5 mmol/kg), reflecting that the fish oil was fresh and almost no oxidative deterioration. In brief, the physicochemical quality of Pacific saury was in good quality.

3.2. FAs composition

FAs composition is one of the most significant indicators for the evaluation of lipid quality. FAs are important components of cell membranes, and the higher the degree of unsaturation of FAs, the stronger their antioxidant and anti-aging properties (Assmann et al., 2018). The 19 FAs were detected in Pacific saury (Table 1), of which 8 main characteristic FAs were identified: myristic acid: C14:0; palmitic acid, C16:0; oleic acid, C18:1; eicosenoic acid, C20:1; eicosadienoic acid, C20:2; dodecanoic acid, C22:1and eicosapentaenoic acid, C20:5 (EPA); docosahexenoic acid, C22:6(DHA). The relative content of FAs in head, meat, viscera of Pacific saury showed that SFAs, MUFAs, and PUFAs accounted for 21.28%–22.68%, 36.24%–44.52% and 33.14%–41.08%, respectively. PUFAs were significantly higher than that in head,
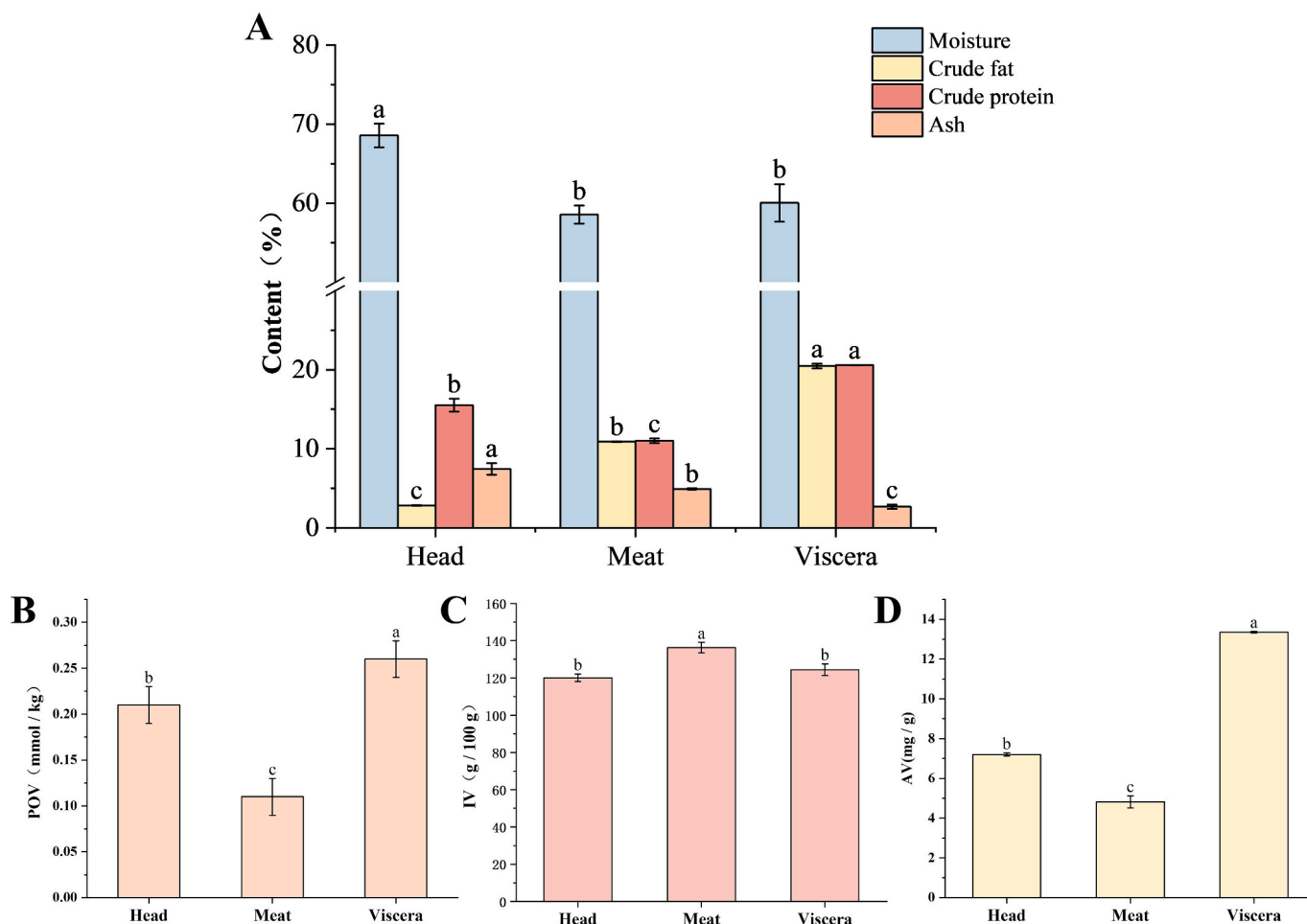
Fig. 1. Nutritional components and physicochemical indexes of different parts of *Cololabis saira*. A) approximate composition, B) acid value, C) iodine value, D) peroxide value. Different superscripts a, b, c values in the same row with different letters differ significantly (*P* < 0.05).

MUFAs were significantly lower compared to meat and viscera(p<0.05). The SFAs, MUFAs, and PUFAs in Burchell's shoulder-hole Antarctic fish (*Trematomus bernacchii*) accounted for 19.4%, 54.4% and 26.0%, respectively (Araujo et al., 2021), while in king salmon (*Oncorhynchus tshawytscha*) accounted for 18%–25%, 28%–51%, and 20%–25%, respectively (Ahmmed et al., 2021).

PUFAs are recognized for their vital nutritional value and regulation of oxidative stress, including modulation of lipid metabolism, mitigation of neurotoxicity and improvement of cognitive performance (Ahmmed et al., 2020). EPA and DHA could promote neural development, improve neurocognitive cell activity (Manual Kollareth et al., 2020), reduce blood lipids, and exhibit cardiovascular and anti-tumor physiological functions (Cheng et al., 2020). The DHA content was significantly higher in head (26.23%) than that in meat (20.91%) and viscera (19.28%), and the EPA content was also significantly higher in viscera (6.97%) and head (6.75%) than that in meat (6.12%)(p<0.05). Particularly, the EPA + DHA content (32.98%) and the total n-3 PUFAs content in head (34.58%) were significantly higher than that in meat and viscera (p<0.05). Therefore, the quality of FAs in head was better than viscera and meat. Moreover, lipids had favorable health effects when the UFA/SFA ratio was higher than 0.7(Rincón-Cervera et al., 2019). The UFA/SFA of the head, meat and viscera were 3.42, 3.71 and 3.48, respectively, which were much higher than 0.7, proving that Pacific saury is a good source of active lipids.

3.3. Lipidomic profile of fish oil

The LC-MS analysis technique is used to detect the subclasses of lipid compounds as well as the composition of lipid molecular species in fish oil in both positive and negative ion modes, which ensures the completeness and reliability of the lipidomic data. The detection of QC samples could generally respond to the lipid composition of crude fish oil from three different parts, and the total ion flow diagrams and the lipid composition of fish oil are shown in Fig. 2. The results showed that the density and corresponding intensity of the peaks in the positive-ion mode and negative-ion mode, and the different lipid compounds could be exuded and separated and recognized within 24 min. A total of 6 lipid classes and 42 lipid subclasses, amounting to 5752 lipid molecular species, were detected from the three parts.

Lipids composition analysis allowed an overall examination of the range of major lipid composition and content distribution of the samples. The lipid contents of the three parts of Pacific saury were shown (Fig. 2B) as followed: GL (65.07%–79.35%), GP (13.85%–27.90%), SP (3.64%–8.63%), FA (0.72%–1.54%), ST (0.06%–0.29%) and PreL (0.03%–0.14%). Besides, the numbers of each lipid classes were shown (Fig.S1) as followed: GP (2622 lipids, 45.58%), GL (1975 lipids, 34.34%), SP (1019 lipids, 17.72%), FA (103 lipids, 1.79%), ST (30 lipids, 0.52%), and PreL (3 lipids, 0.05%). There were five classes that GL (50.54%–60.75%), GP (19.25%–26.53%), SP (10.94%–12.86%), SL (4.72%–5.85%) and FA (4.34%–6.04%) were identified in the meat, head and viscera of tilapia (*Oreochromis niloticus*), respectively (He et al., 2021). A total of 615 lipids were detected in turbot fillets, of which the

Table 1
Fatty acid composition in different parts of *Cololabis saira* (%).

FAs		tissue		
		Head	Meat	Viscera
C14:0	Myristic Acid	6.43 ± 0.44[b]	7.13 ± 0.33[a]	7.44 ± 0.22[a]
C15:0	Pentadecanoic Acid	0.66 ± 0.07[a]	0.58 ± 0.04[a]	0.60 ± 0.02[a]
C16:0	Palmitic Acid	12.43 ± 0.13[a]	11.03 ± 0.52[a]	11.60 ± 0.30[a]
C16:1	Palmitoleic Acid	2.60 ± 0.14[a]	2.48 ± 0.15[a]	2.71 ± 0.10[a]
C17:0	Heptadecanoic Acid	0.55 ± 0.09[a]	0.46 ± 0.02[a]	0.49 ± 0.01[a]
C18:0	Stearic Acid	2.39 ± 0.43[a]	1.86 ± 0.11[a]	1.97 ± 0.03[a]
C18:1N9C	Oleic Acid	4.69 ± 0.83[a]	3.78 ± 0.16[a]	4.21 ± 0.13[a]
C18:2N6C	Linoleic Acid	1.59 ± 0.07[a]	1.54 ± 0.08[a]	1.68 ± 0.04[a]
C20:0	Arachidonic Acid	0.22 ± 0.02[b]	0.22 ± 0.01[b]	0.23 ± 0.00[a]
C18:3 N3	Linolenic Acid	1.31 ± 0.06[a]	2.15 ± 1.54[a]	1.43 ± 0.05[a]
C20:1	Eicosenoic Acid	10.83 ± 3.11[b]	15.11 ± 1.54[a]	15.17 ± 0.37[a]
C20:2	Eicosadienoic Acid	3.75 ± 0.23[a]	3.00 ± 2.41[a]	3.10 ± 2.48[a]
C20:3 N3	Eicosatrienoic Acid	0.29 ± 0.07[a]	0.22 ± 0.05[a]	0.28 ± 0.01[a]
C20:4 N6	Arachidonic Acid	0.46 ± 0.12[a]	0.32 ± 0.02[a]	0.36 ± 0.01[a]
C22:1	Dodecanoic Acid	17.60 ± 3.59[a]	21.14 ± 1.14[a]	22.08 ± 0.82[a]
C22:2	Docosadienoic Acid	0.70 ± 0.54[a]	0.69 ± 0.59[a]	0.05 ± 0.05[a]
C20:5 (EPA)	Eicosapentaenoic Acid	6.75 ± 0.53[ab]	6.12 ± 0.35[b]	6.97 ± 0.19[a]
C24:1	Nervonic Acid	0.52 ± 0.35[a]	1.25 ± 0.76[a]	0.35 ± 0.36[a]
C22:6 (DHA)	Docosahexenoic Acid	26.23 ± 4.25[a]	20.91 ± 1.33[b]	19.28 ± 0.54[b]
Saturated Fatty Acids (SFA)		22.68 ± 1.58[a]	21.28 ± 1.00[a]	22.34 ± 0.55[a]
Unsaturated Fatty Acids (UFA)		77.32 ± 1.58[a]	78.72 ± 1.00[a]	77.66 ± 0.55[a]
Monounsaturated Fatty Acids (MUFA)		36.24 ± 6.10[b]	43.76 ± 1.40[a]	44.52 ± 1.19[a]
Polyunsaturated Fatty Acids (PUFA)		41.08 ± 4.54[a]	34.96 ± 2.34[ab]	33.14 ± 1.75[b]
n-3 Fatty Acids		34.58 ± 4.91[a]	29.40 ± 1.59[b]	27.95 ± 0.78[ab]
n-6 Fatty Acids		2.06 ± 0.19[a]	1.86 ± 0.10[a]	2.04 ± 0.05[a]
UFA/SFA		3.42 ± 0.32[a]	3.71 ± 0.22[a]	3.48 ± 0.11[a]
EPA + DHA		32.98 ± 4.78[a]	27.03 ± 1.68[b]	26.25 ± 0.73[b]

Different superscripts a, b, c values in the same row with different letters differ significantly (P < 0.05).
Note: C18:1N9C, *cis*-9-Octadecenoic acid methyl ester; C18:2N6C, *Cis*-9.12-Octadecedienoic Methyl ester.

most numerous was GL (208 lipids, 33.82%) (Xu et al., 2022). GL and GP in *oyster Crassostrea gigas* was account for 64.08%–78.92% and 11.46%–29.28% of the whole lipid (Liu, Zhao, et al., 2022). It could be seen that GL were the predominant lipid in other aquatic products while GP were the most abundant lipid in Pacific saury.

The relative content of GP subclasses in head, meat and viscera of Pacific saury were shown(Fig. 2C) as followed: 10.90%, 7.38%, and 6.00% of PC; 5.64%, 3.59%, and 2.69% of phosphatidylethanolamine (PE); 4.45%, 1.67%, 2.07% phosphatidylglycerol (PG); 3.07%, 0.92%, 1.21% phosphatidylserine (PS); 2.24%, 1.23%, 1.03% phosphatidylinositol (PI); 1.41%, 1.07%, 0.52% lysophosphatidylcholine (LPC);

0.09%, 0.30%, 0.25% lysodimethylphosphatidylethanolamine (LPE); 0.06%, 0.03%, 0.05% (phosphatidic acid, PA) and 0.01%, 0.01%, 0.03% lysophosphatidylserine (LPS), respectively. 1699 lipids of 32 classes lipids were detected in the hepatopancreas of *Penaeus vannamei* by LC-MS/MS analysis. Among them, 28.21% PC and 11.60% PE were contained (Duan et al., 2022). PC 14.30 mg/g, PE 8.20 mg/g, PI 1.60 mg/g, and PS 9.83 mg/g were identified in pike crab (Zhang, Zhang, et al., 2022). In addition, it is worthwhile to point out that lysophospholipids (LPLs), such as LPC, LPE, LPG, LPA, LPS were found in different parts of Pacific saury, which was less reported in previous studies of aquatic product. LPL is single-chain fatty acyl phospholipid derivatives resulting from the hydrolysis or enzymatic hydrolysis of phospholipid *Sn*-1 or *Sn*-2 position (Xie et al., 2020). LPLs have better emulsifying properties and special biological activities compared with PLs, could participate in signaling processes in physiological functions, regulate the physiological metabolism of the body and improve lipid metabolism and related diseases (Yuan et al., 2024).

3.4. Differential expression of lipid molecules

When performing significance analysis different groups of samples, commonly used univariate statistical analysis methods include Fold Change Analysis and *t*-test. In order to further compare the differences between the lipid molecular species of the three parts of Pacific saury, this test was based on univariate analysis of variance for all detected lipid molecules. The differential lipids in the results of this test were determined by simultaneously satisfying $p < 0.05$ in the t-test and Variable Importance Projection (VIP) > 1 in the OPLS-DA model, and $P_{adj} < 0.05$ and log_2Fold Change >1 were used as criteria for significance of differences in the volcano plot.

Venn plots is performed to visualize how many significant difference lipid molecules change across different comparison groups, which could help to screen key lipid molecule modules related to biological processes (Deng et al., 2022). As shown in Fig. 3A, 132 differential lipids were simultaneously present in the three comparison groups. Among them, there were 101 differential lipids specific to the head_*vs*_meat group, which turned out to be similar to the 110 in the meat_*vs*_viscera group, and both were higher than the 57 in the head_*vs*_viscera group. In addition, a total of 294 differential lipids were expressed in both head_*vs*_meat and head_*vs*_viscera group, 139 differential lipids were expressed in both head_*vs*_viscera and meat_*vs*_viscera group and 83 differential lipids were expressed in both head_*vs*_ and meat_*vs*_viscera group. This suggests that there exist differential lipid molecules of three parts, with smaller differences in the lipid molecules of meat and viscera representing a more similar lipid composition between two groups, while greater variability in the lipid composition of head.

Bubble map is also a form of expressing significant difference lipid molecules. As shown (Fig. 3B) that the differential lipids in the head_*vs*_meat group were mainly triacylglycerol (TG) and diacylglycerol (DG) in the GL; PC, PE, PS, PI, PG in the GP and hexosyl ceramide (Hex1Cer) in the SP. In the head_*vs*_viscera group the differential lipids were mainly TG and DG in the GL; PC, PE, PG, PS in the GP and Hex1Cer in the SP. In the meat_*vs*_viscera group, the differentiated lipids were mainly TG and DG in the GL; PC, PE in the GP and Ceramides (Cer) in the SP. In summary, TG, PC, and PE being the most significantly differentiated lipids present in all tissue.

As shown in Fig. 3C, a total of 2705 differential lipids were shown in the head_*vs*_meat group, of which 1859 were up-regulated and 846 were down-regulated. The results showed that the lipids with the most significant differences between the two sites are mainly the PC and PE in GP. A total of 2481 differential lipids are shown in the head_*vs*_viscera group, of which 1258 are up-regulated and 1223 are down-regulated. The most significant difference between the two sites was the PC in GP. A total of 2263 differential lipids were shown in the meat_*vs*_viscera group, of which 642 were up-regulated and 1621 were down-regulated. The most significant differences between the two sites were Cer in SP
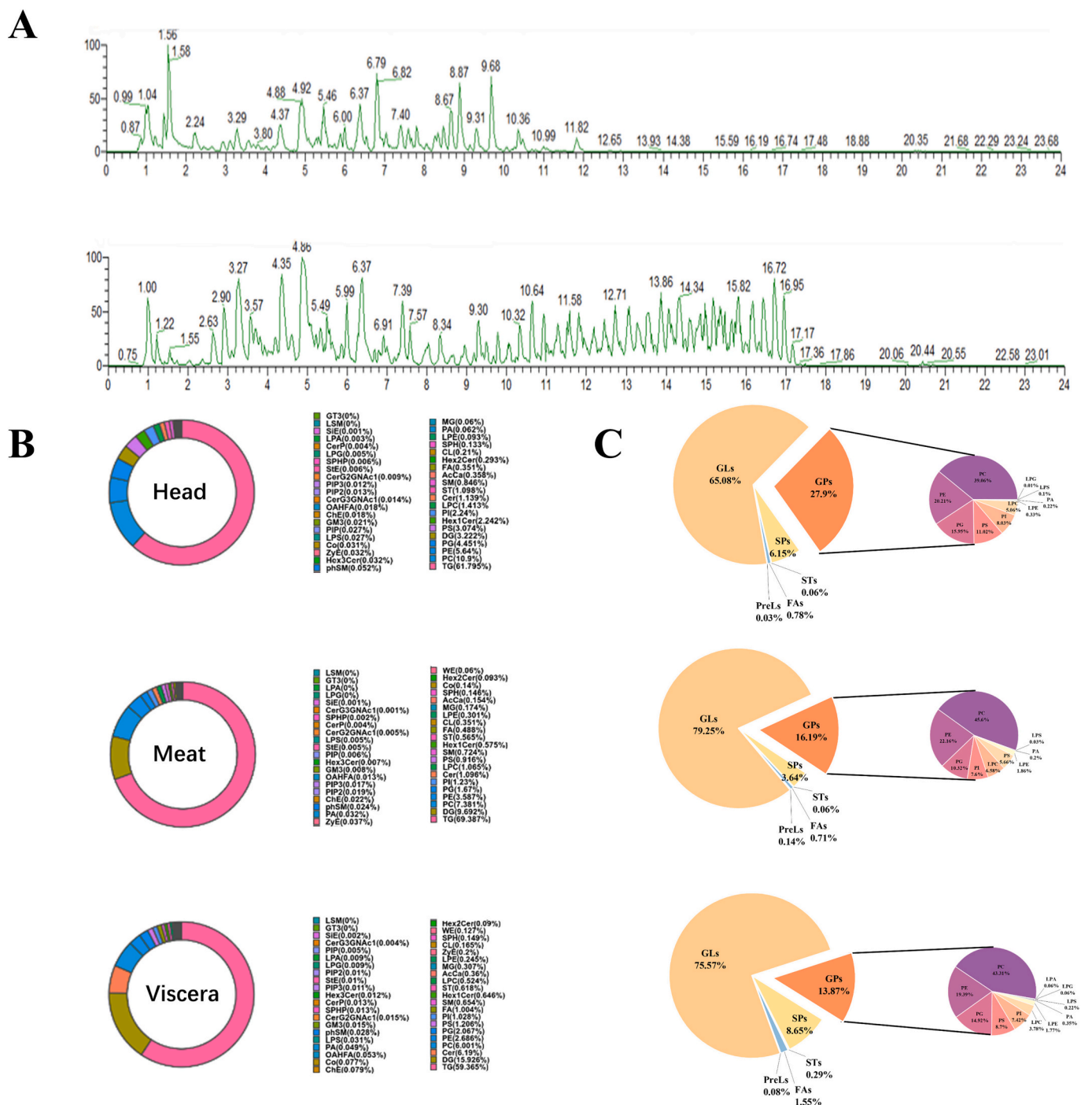
Fig. 2. Lipidomic profile of fish oil. A) Total ion chromatograms of the QC samples obtained in negative and positive ion modes, B) lipid subclasses in different parts of *Cololabis saira*, C) Contents of lipid categories and GPs in *Cololabis saira*. Abbreviation: GPs, glycerophospholipids; GLs, glycerolipids; FAs, fatty acyls; SPs, sphingolipid; STs, sterol lipids; PreLs, prenol lipids.

and PE in GP. Combined with the previous lipid subclass content in each part (Fig. 2B), this may be due to the fact that heads contain higher levels of PC and PE, and viscera contain higher levels of Cer.

It was concluded that PC is the main differential lipid in fish oil. Therefore, analyzing and identifying PC molecular species in fish oil from different parts of Pacific saury may help to obtain comprehensive information of lipid profiles. Non-targeted histological analyses are numerous and complex, and multivariate analysis is a common method for screening key markers (Rocchetti et al., 2018). Orthogonal Partial Least Squares Discrimination Analysis (OPLS-DA) combines orthogonal signal correction technique on the basis of PLS—DA, which helps

filtering out the noise that is not related to the classification information, and improve the parsing ability and effectiveness of the model (Boccard & Rutledge, 2013). The OPLS-DA model (Fig. 3D) showed that the information of the samples in head, meat and viscera groups could be clearly separated, indicating that there is a significant difference between different parts of the Pacific saury. Among them, meat and viscera were closer to each other, representing a similar lipid composition, which provided a basis for subsequent lipidomic analysis.

In order to further express the differential PC molecules in the three parts, differential lipids were screened out the by building discriminant models. The VIP values of the first principal component of OPLS-DA are
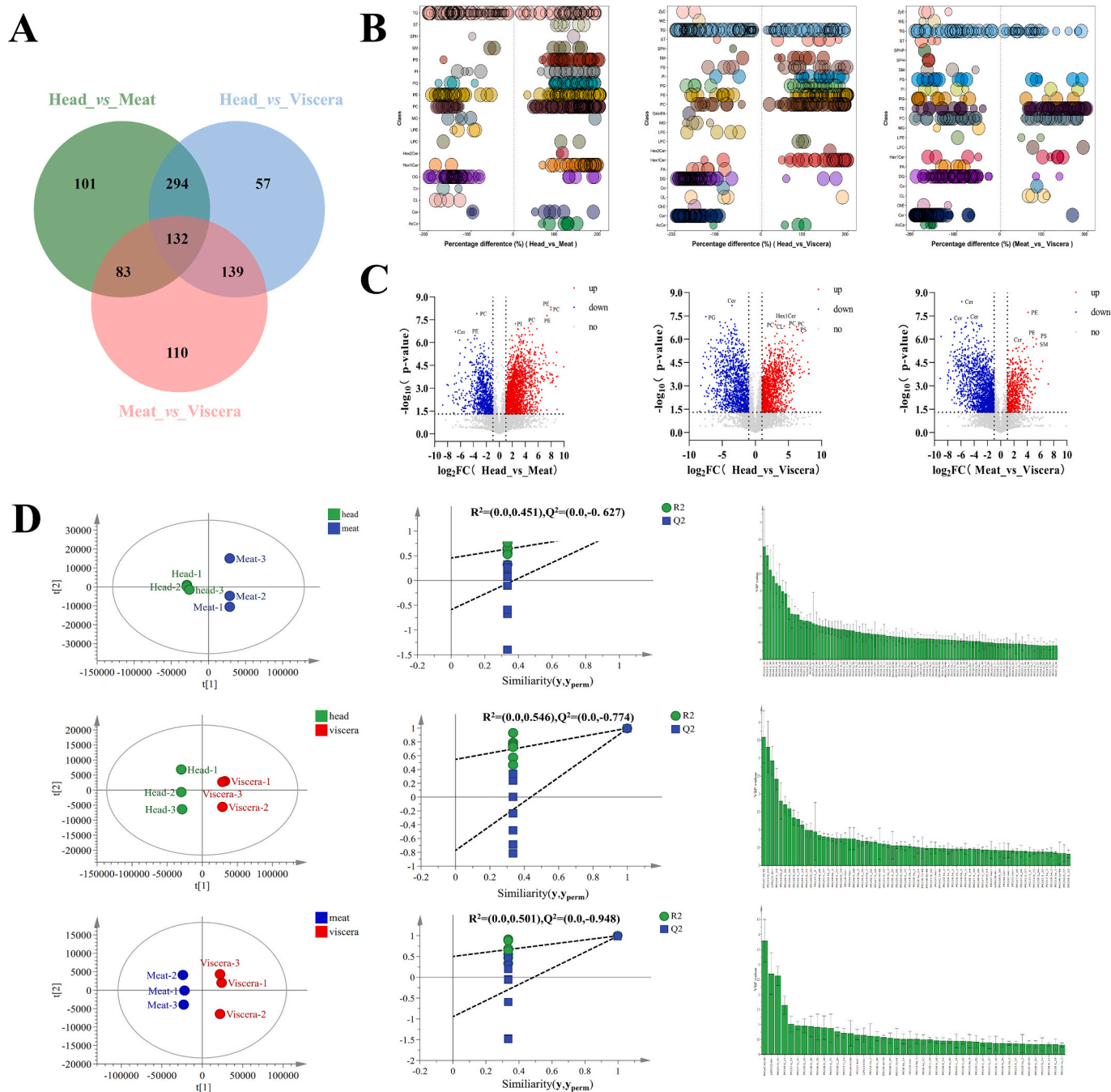
Fig. 3. Characteristic expression of lipid molecules in fish oil. A) Venn graph, B) Bubble plot, C) Volcano graph, D) Multivariate statistical analysis (OPLS-DA graph, Permutation plot, VIP value graph). *Note: In the bubble plot, the vertical coordinate represents each lipid subclass, differentiated by different colors; the size of bubbles represents the significance of the difference, smaller bubbles indicate significant difference ($0.01 < p$ value<0.05), larger bubbles indicate highly significant difference (p value<0.01).

presented in Fig. 3D, and the results show that there were 97,73 and 47 significantly different lipids contained in the three comparison groups, respectively.

This study also enumerated the top 15 characteristic PC in terms of VIP value score, and the results are shown in the Table.S1 and Fig.S2 Among them, PC (14:0_14:0) (VIP = 7.5898), PC (15:0_22:6) (VIP = 7.2120), PC (16:1_16:1) (VIP = 6.1232), PC (16:1_14:0) (VIP = 5.5671), PC (16:0_18:1) (VIP = 5.4759) are significantly characteristic PC in the head_*vs*_meat group; PC (20:3_22:6) (VIP = 10.431), PC (14:0_14:0) (VIP = 8.5753), LPC (22:6) (VIP = 8.4392), PC (16:1_14:0) (VIP = 6.2686), PC (10:0_16:0) (VIP = 5.1730) are significantly characteristic PC in the head_*vs*_viscera group; PC (20:3_22:6) (VIP = 12.101), LPC

(22:6) (VIP = 8.6255), PC (15:0_22:6) (VIP = 8.3446), PC (19:0_14:3) (VIP = 5.2403), PC (15:0_18:1) (VIP = 3.2473) are significantly characteristic PC in the meat_*vs*_viscera group. For the purpose of avoiding overfitting of the supervised model in the modeling process, the Permutation test was used to test the model to ensure the validity of the model (Malzahn et al., 2022). Fig. 3-D showed ($R^2 = 0.0,0.451$), ($Q^2 = 0.0, -0.627$) in head_*vs*_meat group; ($R^2 = 0.0,0.546$), ($Q^2 = 0.0, -0.774$) in head_*vs*_viscera group; ($R^2 = 0.0,0.501$), ($Q^2 = 0.0, -0.948$) in meat_*vs*_viscera group. In brief, with the replacement retention gradually decreasing, the R^2 and Q^2 of the stochastic model are both gradually decreasing, which indicates that the original model does not have the phenomenon of overfitting, the model is well robust.

The top 50 PC in terms of relative contents were listed in Table 2, the result showed that three parts of the Pacific saury were not exactly the same but all of them had the characteristics of linking the long-chain fatty acids, especially the DHA/EPA. The most abundant lipid molecule species in both head and body meat was PC (20:3_22:6), containing 14.59% and 19.60%, respectively, and its content in viscera was the second highest, containing about 10.01%. This PC molecule links C20:3 N3 (Eicosanoid) and C 22:6 (DHA), both n-3 fatty acids. It has been shown that most of EPA and DHA in Atlantic salmon oil is esterified to the *Sn*-2 position (Ruiz-Lopez et al., 2015); the n-3 fatty acid content at the *Sn*-2 position in king salmon roe is also significantly higher than in the skin and head (Ahmmed et al., 2021). The bio-accessibility of fatty acids is related to their positions in the molecular structure of linked phospholipids, and the *Sn*-2 position is more beneficial to the digestion and absorption of fatty acids compared to the *Sn*-1,3 position (Yalagala et al., 2019).

Table 2
PCs with their relative content of different parts (%).

	Head	Meat	Viscera
PC (20:3_22:6)	14.59 ± 1.98	19.60 ± 2.36	10.01 ± 2.14
LPC (22:6)	9.43 ± 1.39	11.06 ± 0.53	6.33 ± 0.63
PC (44:12)	6.25 ± 7.40	5.38 ± 9.29	4.17 ± 7.00
PC (42:2)	5.51 ± 4.79	0.01 ± 0.00	N.D.
PC (10:0_6:0)	3.77 ± 0.60	2.20 ± 0.42	2.74 ± 0.3
PC (20:1_22:1)	3.31 ± 2.82	N.D.	N.D.
PC (16:0_22:6)	3.21 ± 1.10	3.13 ± 0.39	4.23 ± 0.64
PC (16:0_18:1)	2.59 ± 0.51	0.47 ± 0.11	1.51 ± 0.03
PC (18:0_16:0)	2.29 ± 0.38	0.83 ± 0.02	1.83 ± 0.21
PC (20:2_22:6)	1.61 ± 1.37	0.01 ± 0.00	0.02 ± 0.00
PC (14:0_14:0)	1.51 ± 0.28	8.63 ± 3.46	14.29 ± 1.33
PC (16:0_20:5)	1.26 ± 0.29	0.86 ± 0.14	1.99 ± 0.04
PC (18:1_24:1)	1.14 ± 0.10	0.16 ± 0.03	0.08 ± 0.00
PC (16:0_20:1)	1.07 ± 0.25	0.4 ± 0.08	0.70 ± 0.09
PC (22:6_22:6)	1.01 ± 0.23	1.13 ± 0.17	0.57 ± 0.07
PC (18:1_24:0)	0.87 ± 0.18	0.12 ± 0.02	0.03 ± 0.00
PC (20:1_20:5)	0.75 ± 0.14	0.64 ± 0.09	0.73 ± 0.03
PC (16:0_20:5)	0.72 ± 0.11	0.60 ± 0.07	1.57 ± 0.26
PC (35:1_9:0)	0.70 ± 0.44	0.05 ± 0.01	0.06 ± 0.04
LPC (16:0)	0.69 ± 0.14	0.27 ± 0.13	0.39 ± 0.04
PC (16:1_16:1)	0.67 ± 0.08	5.06 ± 1.55	4.24 ± 0.12
PC (16:1_14:0)	0.65 ± 0.14	4.46 ± 2.09	7.32 ± 0.35
PC (16:0_16:1)	0.64 ± 0.14	0.10 ± 0.03	0.27 ± 0.01
PC (38:5e)	0.64 ± 0.11	0.12 ± 0.02	0.41 ± 0.09
PC (16:1_16:1)	0.55 ± 0.21	0.08 ± 0.03	0.25 ± 0.05
PC (34:3e)	0.53 ± 0.07	0.24 ± 0.04	0.24 ± 0.19
PC (20:2e_23:0)	0.50 ± 0.18	1.44 ± 0.80	1.09 ± 0.06
PC (18:1_18:1)	0.49 ± 0.07	0.10 ± 0.02	0.32 ± 0.02
PC (20:5_22:6)	0.46 ± 0.61	0.57 ± 0.55	0.47 ± 0.32
PC (32:1_22:6)	0.45 ± 0.10	N.D.	0.02 ± 0.00
PC (40:9)	0.43 ± 0.07	0.52 ± 0.05	1.14 ± 0.22
PC (18:1_22:6)	0.43 ± 0.08	0.33 ± 0.06	0.59 ± 0.01
PC (18:1_22:1)	0.43 ± 0.12	0.07 ± 0.01	0.07 ± 0.00
PC (20:1e_22:6)	0.43 ± 0.05	0.03 ± 0.01	0.03 ± 0.00
PC (16:0_24:1)	0.41 ± 0.10	0.04 ± 0.01	0.04 ± 0.00
PC (18:0e_18:1)	0.40 ± 0.09	0.02 ± 0.00	0.02 ± 0.01
PC (16:0_16:0)	0.38 ± 0.06	0.05 ± 0.02	0.29 ± 0.01
PC (16:1_20:5)	0.38 ± 0.07	0.18 ± 0.04	0.82 ± 0.01
PC (18:2e_22:6)	0.37 ± 0.12	0.02 ± 0.00	0.05 ± 0.00
PC (19:0_14:3)	0.36 ± 0.03	2.86 ± 0.56	0.81 ± 0.06
PC (18:1_22:6)	0.35 ± 0.09	0.18 ± 0.01	0.24 ± 0.01
PC (20:5_22:6)	0.34 ± 0.06	0.53 ± 0.08	0.64 ± 0.02
PC (16:0e_18:1)	0.34 ± 0.08	0.02 ± 0.00	0.05 ± 0.00
PC (36:4)	0.33 ± 0.06	0.17 ± 0.00	0.53 ± 0.01
PC (42:7)	0.32 ± 0.28	0.77 ± 1.29	0.02 ± 0.02
PC (38:5e)	0.32 ± 0.04	0.26 ± 0.03	0.43 ± 0.06
PC (15:0_22:6)	0.31 ± 0.04	5.95 ± 0.81	0.51 ± 0.07
PC (16:1_22:6)	0.30 ± 0.06	0.18 ± 0.04	0.53 ± 0.01
PC (17:1_18:1)	0.30 ± 0.06	0.02 ± 0.00	0.03 ± 0.00
PC (16:0_14:0)	0.30 ± 0.06	0.05 ± 0.02	0.28 ± 0.01

Note: Relative Content: R. C.

3.5. Correlation analysis

Different fatty acids were linked to the phospholipid skeleton constituting different PC molecules, and in order to further investigate the effect of differences in microscopic molecular composition on macroscopic properties (AV, IV, POV), correlation analysis was applied to investigate the connection among them. The correlation heatmap of characteristic PC molecules in different comparison groups (Fig. 4A) showed that the relative abundance of characteristic PC molecules in meat was lower than that in the head and viscera. Meanwhile the characteristic PC molecular species had the highest abundance in the head_*vs*_viscera group.

Fig. 4B visualizes their correlation by constructing a neural network diagram. Most of these indicators were only associated with three parts of Pacific saury (head, meat and viscera), however, it is worth pointing out that PC (18:1_22:6), PC (16:1_20:5), PC (16:0_20:5), PC (16:1_16:1), PC (18:2_16:0), PC (36:4), PC (38:5) have higher degree coefficients. The Person correlation analysis method was further performed to analyze their correlations (Fig. 4C), this study additionally enumerates PC-DHA/EPA, result showed that PC (18:1_22:6) had significant positive correlation with PC36:4 ($R = 0.9986$), PC (16:1_20:5) ($R = 0.9954$), AV ($R = 0.9918$) while significant negative correlation with C20:5 ($R = -0.9689$). PC (16:0_20:5) has significant positive correlations with PC (18:1_22:6) ($R = 0.9989$), PC (16:1_20:5) ($R = 0.9987$), AV ($R = 0.9967$), PC (36:4) ($R = 0.99516$), and significant negative correlations existed with C20:5 ($R = -0.9565$). PC (16:1_20:5) showed significant positive correlation with AV ($R = 0.9994$) and significant negative correlation with C20:5 ($R = -0.9410$). It may be concluded that PC-DHA/EPA may be associated with AV.

4. Conclusion

This study detected the Pacific saury's FAs composition and lipid profiles by using GC and UPLC-ESI-MS/MS. Head had a low lipid yield, but nutritionally rich in PUFAs (especially EPA and DHA); meat and viscera could be further exploited due to the high contents of lipids and FAs. GP were the most numerous fraction (45.58%) in Pacific saury lipids, with PC being the main differential subclass. 18 characteristic differential lipids in the head and meat were identified, 15 of which were differential lipids in the head and viscera. PC (14:0_14:0), PC (15:0_22:6) and PC(16:1_16:1) were the characteristic PC in the head_-*vs*_meat group; PC (20:3_22:6), PC (14:0_14:0) and LPC (22:6) were characteristic PC in the head_*vs*_viscera group; PC (20:3_22:6), LPC (22:6) and PC (15:0_22:6) were the characteristic PC in the meat_*vs*-viscera group. The characteristic PC had the highest abundance in the head_*vs*_viscera group. PC-DHA/EPA may be associated with AV. This study provides an in-depth exploration of lipid profiles of Pacific saury, which could provide theoretical basis for further processing of its by-products and lipid utilization.

CRediT authorship contribution statement

Xinyi Tao: Writing – review & editing, Writing – original draft, Methodology, Investigation, Formal analysis, Data curation, Conceptualization. **Mingyu Yin:** Writing – review & editing, Software, Data curation. **Liu Lin:** Methodology, Formal analysis. **Rongzhen Song:** Software, Methodology, Investigation. **Ningping Tao:** Writing – review & editing, Visualization, Supervision, Resources. **Xichang Wang:** Resources, Project administration.

Declaration of competing interest

The authors declare that they have no known competing financial interests or personal relationships that could have appeared to influence the work reported in this paper.
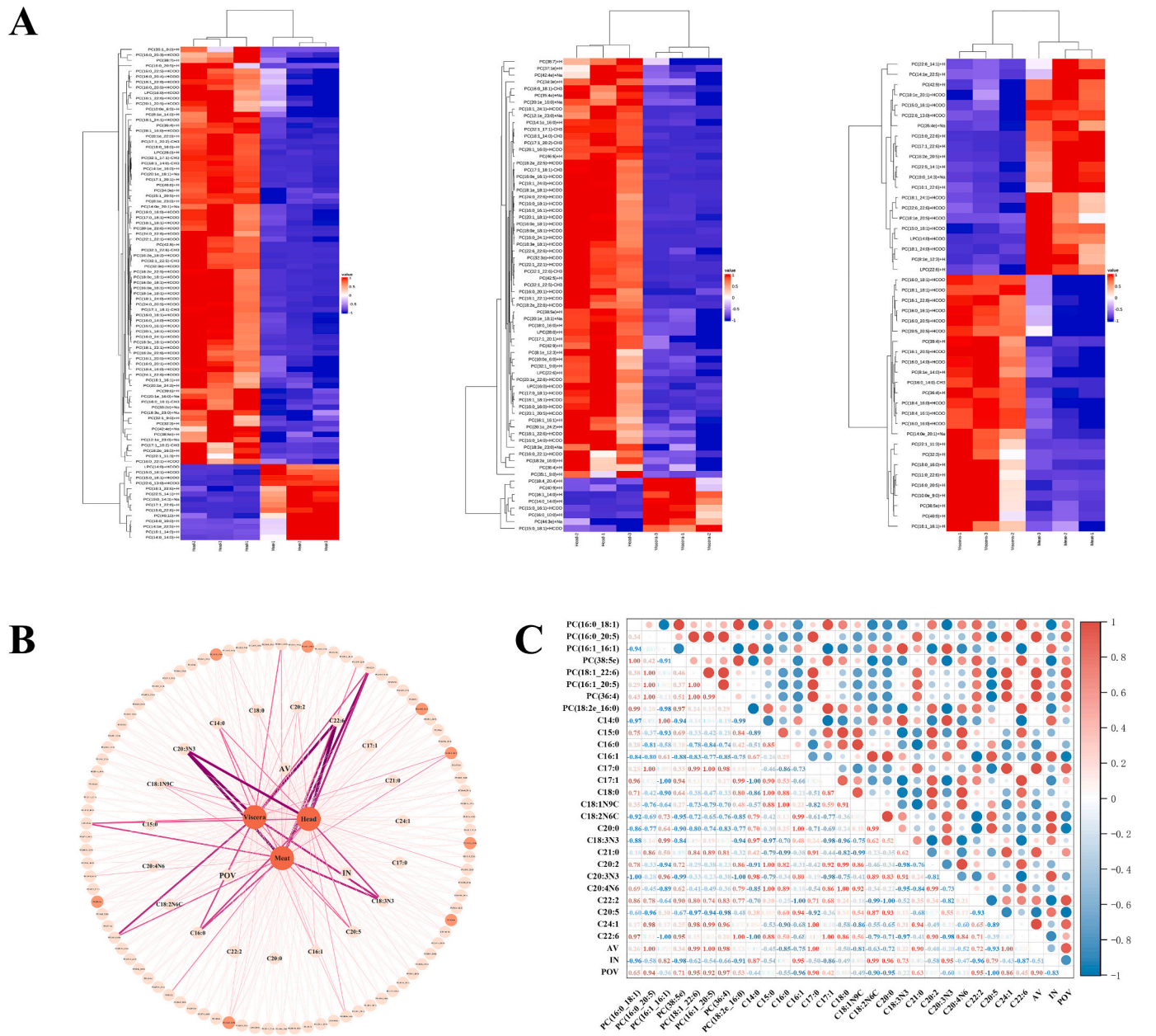
A

B

C

Fig. 4. Correlation analysis between differential PC and FAs, physical and chemical indicators in different parts. A) Clustering heat map (head_*vs*_meat group, head_*vs*_viscera group, meat_*vs*_viscera group), B) Neural network diagram, C) Correlation heat map. *Note: The shade of the icon color represents the level of degree coefficient and the thickness of the line reflects the level of content.

Data availability

Data will be made available on request.

Acknowledgements

Appendix A. Supplementary data

Supplementary data to this article can be found online at https://doi.org/10.1016/j.fochx.2024.101682.

References

Ahmmed, M. K., Ahmmed, F., Tian, H., Sabrina Carne, A., & Bekhit, A. E.-D. (2020). Marine omega-3 (n-3) phospholipids: A comprehensive review of their properties, sources, bioavailability, and relation to brain health. *Comprehensive Reviews in Food Science and Food Safety, 19*(1), 64–123. https://doi.org/10.1111/1541-4337.12510

Ahmmed, M. K., Carne, A., Ahmmed, F., Stewart, I., Tian, H., & Bekhit, A. E.-D. A. (2021). Positional distribution of fatty acids and phospholipid composition in king salmon (*Oncorhynchus tshawytscha*) head, roe and skin using nuclear magnetic resonance spectroscopy. *Food Chemistry, 363*, Article 130302. https://doi.org/10.1016/j.foodchem.2021.130302

Araujo, P., Truzzi, C., Belghit, I., & Antonucci, M. (2021). The impact of seawater warming on fatty acid composition and nutritional quality indices of *Trematomus bernacchii* from the Antarctic region. *Food Chemistry, 365*, Article 130500. https://doi.org/10.1016/j.foodchem.2021.130500

Assmann, K. E., Adjibade, M., Hercberg, S., Galan, P., & Kesse-Guyot, E. (2018). Unsaturated fatty acid intakes during midlife are positively associated with later cognitive function in older adults with modulating effects of antioxidant supplementation. *The Journal of Nutrition, 148*(12), 1938–1945. https://doi.org/10.1093/jn/nxy206

Behrouz, V., & Yari, Z. (2022). A review on differential effects of dietary fatty acids on weight, appetite and energy expenditure. *Critical Reviews in Food Science and Nutrition, 62*(8), 2235–2249. https://doi.org/10.1080/10408398.2020.1852172

Bledsoe, G. E., Bledsoe, C. D., & Racso, B. (2003). Caviars and fish roe products. *Critical Reviews in Food Science and Nutrition, 43*(3), 317–356.

Boccard, J., & Rutledge, D. N. (2013). A consensus orthogonal partial least squares discriminant analysis (OPLS-DA) strategy for multiblock omics data fusion. *Analytica Chimica Acta, 769*, 30–39. https://doi.org/10.1016/j.aca.2013.01.022

Chen, J., Kong, Q., Sun, Z. T., & Liu, J. Y. (2022). Freshness analysis based on lipidomics for farmed Atlantic salmon (*Salmo salar L.*) stored at different times. *Food Chemistry, 373*, Article 131564. https://doi.org/10.1016/j.foodchem.2021.131564

Cheng, L. C., Hu, T., Shi, H. L., Chen, X., Wang, H. Q., Zheng, K. Y., Huang, X. F., & Yu, Y. H. (2020). DHA reduces hypothalamic inflammation and improves central leptin signaling in mice. *Life Sciences, 257*, Article 118036. https://doi.org/10.1016/j.lfs.2020.118036

Cui, Y., Wang, H., Zhao, Q., Zhu, X., Wang, P., Xue, J., … Shen, Q. (2021). Real-time detection of authenticity and adulteration of krill phospholipids with soybean phospholipids using rapid evaporative ionization mass spectrometry: Application on commercial samples. *Food Control, 121*, 107680. https://doi.org/10.1016/j.foodcont.2020.107680

Das, U. N. (2018). Arachidonic acid and other unsaturated fatty acids and some of their metabolites function as endogenous antimicrobial molecules: A review. *Journal of Advanced Research, 11*, 57–66. https://doi.org/10.1016/j.jare.2018.01.001

Deng, L., Yang, Y. X., Li, Z., Li, J., Zhu, Y. P., Meng, Q. Z., … Wang, X. F. (2022). Impact of different dietary regimens on the lipidomic profile of mare's milk. *Food Research International, 156*, Article 111305. https://doi.org/10.1016/j.foodres.2022.111305

Dowhan, W. (2017). Understanding phospholipid function: Why are there so many lipids? *Journal of Biological Chemistry, 292*(26), 10755–10766. https://doi.org/10.1074/jbc.X117.794891

Duan, Y. F., Zeng, S. M., Lu, Z. J., Dan, X. M., Mo, Z. Q., Xing, Y. F., … Li, Y. W. (2022). Responses of lipid metabolism and lipidomics in the hepatopancreas of Pacific white shrimp *Litopenaeus vannamei* to microcystin-LR exposure. *Science of the Total Environment, 820*, Article 153245. https://doi.org/10.1016/j.scitotenv.2022.153245

Fang, C. D., Chen, H. S., Yan, H. B., Shui, S. S., Benjakul, S., & Zhang, B. (2022). Investigation of the changes in the lipid profiles in hairtail (*Trichiurus haumela*) muscle during frozen storage using chemical and LC/MS-based lipidomics analysis. *Food Chemistry, 390*, Article 133140. https://doi.org/10.1016/j.foodchem.2022.133140

Ferraris, Q., Alcazar, A., & Qian, M. C. (2022). Profiling polar lipids in whey protein phospholipid concentrate by LC-HRMS/MS. *Food Chemistry, 374*, 131495. https://doi.org/10.1016/j.foodchem.2021.131495

Gao, X. H., Zhang, X. Y., Yu, H. X., & Yu, C. C. (2020). Analysis and evaluation of the nutritional components in the muscle of *Pseudosciaena polyactis* and *collichthys lucidus*. *Journal of Zhejiang University (Science Edition), 47*(3), 362–369. https://doi.org/10.3785/J.JFCA.2021.103885

Haq, M., Suraiya, S., Ahmed, S., & Chun, B.-S. (2021). Phospholipids from marine source: Extractions and forthcoming industrial applications. *Journal of Functional Foods, 80*, Article 104448. https://doi.org/10.1016/j.jff.2021.104448

He, C., Cao, J., Bao, Y. Y., Sun, Z. X., Liu, Z. Y., & Li, C. (2021). Characterization of lipid profiling in three parts (muscle, head and viscera) of tilapia (*Oreochromis niloticus*) using lipidomics with UPLC-ESI-Q-TOF-MS. *Food Chemistry, 347*, Article 129057. https://doi.org/10.1016/j.foodchem.2021.129057

Li, X. B., He, Q. X., Hou, H. R., Zhang, S. S., Zhang, X. M., Zhang, Y., Wang, X. M., Han, L. W., & Liu, K. C. (2018). Targeted lipidomics profiling of marine phospholipids from different resources by UPLC-Q-Exactive Orbitrap/MS approach. *Journal of Chromatography B, 1096*, 107–112. https://doi.org/10.1016/j.jchromb.2018.08.018

Liu, L. L., Luo, M., Liu, H. T., Chen, F. X., & Han, L. (2023). Analysis and evaluation of the muscle nutrition of different sizes of wild yellowfin tuna (*Thunnus albacares*). *Progress in Fishery Sciences, 1–10*. https://doi.org/10.19663/j.issn2095-9869.20230314001

Liu, S. N., Wang, S. N., Cao, R., Zhao, L., & Liu, Q. (2022). Nutritional composition analysis and quality evaluation of different sizes of *Ammodytes personatus*. *Progress in Fishery Sciences, 43*(1), 188–194. https://doi.org/10.19663/j.issn2095-9869.20200825001

Liu, Z. Q., Zhao, M. T., Wang, X. W., Li, C., Liu, Z. Y., Shen, X. R., & Zhou, D. Y. (2022). Investigation of *oyster Crassostrea gigas* lipid profile from three sea areas of China based on non-targeted lipidomics for their geographic region traceability. *Food Chemistry, 386*, Article 132748. https://doi.org/10.1016/j.foodchem.2022.132748

Lordan, R., Tsoupras, A., & Zabetakis, I. (2017). Phospholipids of animal and marine origin: Structure, function, and anti-inflammatory properties. *Molecules, 22*(11). https://doi.org/10.3390/molecules22111964. Article 11.

Malzahn, A. M., Sarno, A., Hagemann, A., Farkas, J., Musialak, L. A., Kjørsvik, E., & Hansen, B. H. (2022). Can lipidomics help identifying egg quality in ballan wrasse? *Aquaculture, 552*, Article 738018. https://doi.org/10.1016/j.aquaculture.2022.738018

Manual Kollareth, D. J., Deckelbaum, R. J., Liu, Z., Ramakrishnan, R., Jouvene, C., Serhan, C. N., … Zirpoli, H. (2020). Acute injection of a DHA triglyceride emulsion after hypoxic-ischemic brain injury in mice increases both DHA and EPA levels in blood and brain. *Prostaglandins, Leukotrienes and Essential Fatty Acids, 162*, Article 102176. https://doi.org/10.1016/j.plefa.2020.102176

Nandi, U., Onyesom, I., & Douroumis, D. (2021). An *in vitro* evaluation of antitumor activity of sirolimus-encapsulated liposomes in breast cancer cells. *Journal of Pharmacy and Pharmacology, 73*(3), 300–309. https://doi.org/10.1093/jpp/rgaa061

Nisticò, N., Greco, M., Bruno, M. C., Giuliano, E., Sinopoli, P., & Cosco, D. (2023). Biomimetic lipid membranes: An overview on their properties and applications.

Applied Materials Today, 35, Article 101998. https://doi.org/10.1016/j.apmt.2023.101998

Ochiai, M., & Komiya, Y. (2021). Detection of edible insect derived phospholipids with polyunsaturated fatty acids by thin-layer chromatography, gas chromatography, and enzymatic methods. *Journal of Food Composition and Analysis, 99*, 103869. https://doi.org/10.1016/j.jfca.2021.103869

Ong, W. Y., Go, M. L., Wang, D. Y., Cheah, I. K. M., & Halliwell, B. (2021). Effects of antimalarial drugs on Neuroinflammation-potential use for treatment of COVID-19-related neurologic complications. *Molecular Neurobiology, 58*(1), 106–117. https://doi.org/10.1007/s12035-020-02093-z

Petenuci, M. E., Lopes, A. P., Camparim, R., Schneider, V. V. A., & Visentainer, J. V. (2021). Fatty acid composition in fractions of neutral lipids and phospholipids of Hemisorubim platyrhynchos with seasonal distinction. *Journal of Food Composition and Analysis, 99*, 103885. https://doi.org/10.1016/j.jfca.2021.103885

Rincón-Cervera, M.Á., González-Barriga, V., Valenzuela, R., López-Arana, S., Romero, J., & Valenzuela, A. (2019). Profile and distribution of fatty acids in edible parts of commonly consumed marine fishes in Chile. *Food Chemistry, 274*, 123–129. https://doi.org/10.1016/j.foodchem.2018.08.113

Rocchetti, G., Gatti, M., Bavaresco, L., & Lucini, L. (2018). Untargeted metabolomics to investigate the phenolic composition of chardonnay wines from different origins. *Journal of Food Composition and Analysis, 71*, 87–93. https://doi.org/10.1016/j.jfca.2018.05.010

Ruiz-Lopez, N., Stubhaug, I., Ipharraguerre, I., Rimbach, G., & Menoyo, D. (2015). Positional distribution of fatty acids in Triacylglycerols and phospholipids from fillets of Atlantic Salmon (*Salmo Salar*) fed vegetable and fish oil blends. *Marine Drugs, 13*(7). https://doi.org/10.3390/md13074255. Article 7.

Song, R. Z., Wang, X. C., Deng, S. G., & Tao, N. P. (2022). Lipidomic analysis and triglyceride profiles of fish oil: Preparation through silica gel column and enzymatic treatment. *Food Research International, 162*, Article 112100. https://doi.org/10.1016/j.foodres.2022.112100

Su, H., Li, Y. X., Qian, X. L., Fan, X. Y., Zhang, J., & Tao, N. P. (2019). Nutrition analysis and quality evaluation of *Aristichthys nobilis*, *Thunnus obesus* and *Salmon Salar* head. *Science and Technology of Food Industry, 40*(17). https://doi.org/10.13386/j.issn1002-0306.2019.17.035, 212–217, 224.

Sun, J. Y., Hu, P. P., Lyu, C. M., Tian, J. L., Meng, X. J., Tan, H., & Dong, W. X. (2022). Comprehensive lipidomics analysis of the lipids in hazelnut oil during storage. *Food Chemistry, 378*, Article 132050. https://doi.org/10.1016/j.foodchem.2022.132050

Tam, J., Ahmad, I. A. H., & Blasko, A. (2018). A four parameter optimization and troubleshooting of a RPLC – charged aerosol detection stability indicating method for determination of S-lysophosphatidylcholines in a phospholipid formulation. *Journal of Pharmaceutical and Biomedical Analysis, 155*, 288–297. https://doi.org/10.1016/j.jpba.2018.03.067

Valencia-Naranjo, A., Manjarres-Correa, L. M., & Bermúdez-Cardona, J. (2022). Pilot study of the effect of EPA + DHA supplementation on the fatty acid profile of erythrocytes and breast milk of lactating women from *Sonsón*, Colombia. *Current Research in Food Science, 5*, 789–797. https://doi.org/10.1016/j.crfs.2022.04.008

Wang, C. C., Kong, J. Y., Li, X. Y., Yang, J. Y., Xue, C. H., Yanagita, T., & Wang, Y. M. (2022). Antarctic krill oil exhibited synergistic effects with nobiletin and theanine in ameliorating memory and cognitive deficiency in SAMP8 mice: Applying the perspective of the sea–land combination to retard brain aging. *Frontiers in Aging Neuroscience, 14*, Article 964077. https://doi.org/10.3389/fnagi.2022.964077

Wang, L., Zhao, L., Qi, X. M., Liu, Q., & Mou, W. L. (2022). Nutritional composition analysis and quality evaluation of muscles of different specifications of *Cololabis saira*. *Journal of Food Safety and Quality, 13*(21), 6815–6820. https://doi.org/10.19812/j.cnki.jfsq11-5956/ts.2022.21.003

Wang, P., Zhong, L. L., Yang, H. B., Zhang, J., Hou, X. J., Wu, C. Y., Zhang, R., & Cheng, Y. J. (2022). Comprehensive comparative analysis of lipid profile in dried and fresh walnut kernels by UHPLC-Q-Exactive Orbitrap/MS. *Food Chemistry, 386*, Article 132706. https://doi.org/10.1016/j.foodchem.2022.132706

Wang, X. (2023). International fisheries dynamics. *Fishery Information & Strategy, 38*(4), 317–324.

Wang, X. Y., Xie, J., & Chen, X. J. (2021). Differences in lipid composition of bigeye tuna (*Thunnus obesus*) during storage at 0 °C and 4 °C. *Food Research International, 143*, Article 110233. https://doi.org/10.1016/j.foodres.2021.110233

Xie, Y., Wu, B. F., Wu, Z. Y., Tu, X. H., Xu, S. L., Lv, X., Yin, H. Q., Xiang, J. Q., Chen, H., & Wei, F. (2020). Ultrasound-assisted one-phase solvent extraction coupled with liquid chromatography-quadrupole time-of-flight mass spectrometry for efficient profiling of egg yolk lipids. *Food Chemistry, 319*, Article 126547. https://doi.org/10.1016/j.foodchem.2020.126547

Xu, H. G., Luo, X., Wei, Y. L., & Liang, M. Q. (2022). Dietary lysophosphatidylcholine regulates diacylglycerol, cardiolipin and free fatty acid contents in the fillet of turbot. *Food Chemistry: X, 14*, Article 100293. https://doi.org/10.1016/j.fochx.2022.100293

Yaghmour, M. H., Thiele, C., & Kuerschner, L. (2021). An advanced method for propargylcholine phospholipid detection by direct-infusion MS. *Journal of Lipid Research, 62*, 100022. https://doi.org/10.1016/j.jlr.2021.100022

Yalagala, P. C. R., Sugasini, D., Dasarathi, S., Pahan, K., & Subbaiah, P. V. (2019). Dietary lysophosphatidylcholine-EPA enriches both EPA and DHA in the brain: Potential treatment for depression[S]. *Journal of Lipid Research, 60*(3), 566–578. https://doi.org/10.1194/jlr.M090464

Ye, B. Q., Tao, N. P., Wang, X. C., & Zhu, Q. C. (2013). Research progress in nutritional evaluation , storage and processing of *Cololabis saira* and comprehensive utilization of its processing by-products. *Science and Technology of Food Industry, 34*(22). https://doi.org/10.13386/j.issn1002-0306.2013.22.013, 367–370, 374.

Yin, M., Luo, G., Matsuoka, R., Zhao, Y., Long, Z., Zhou, F., & Wang, X. C. (2024). Metabolic effects of phospholipids extracted from capelin (*Mallotus villosus*) roe on

HepG2 cells. *Food Bioscience, 59*, Article 104257. https://doi.org/10.1016/j.fbio.2024.104257

Yin, M. Y., Chen, M., Yanagisawa, T., Matsuoka, R., Zhang, L., Qiu, W. Q., Tao, N. P., Xi, Y. C., & Wang, X. C. (2022). A comparative study on the nutritional evaluation of the head, meat, roe, and viscera of rainbow smelt (*Osmerus mordax*). *Journal of Food Composition and Analysis, 109*, Article 104469. https://doi.org/10.1016/j.jfca.2022.104469

Yuan, C. C., Xu, Y., Lu, G. T., Hu, Y. P., Mao, W. J., Ke, L., Tong, Z. H., Xia, Y., Ma, S. S., Dong, X. Y., Xian, X. D., Wu, X. B., Liu, G., Li, B. Q., & Li, W. Q. (2024). AAV-mediated hepatic expression of LPL ameliorates severe hypertriglyceridemia and its related acute pancreatitis in Gpihbp1 deficient mice and rats. *Molecular Therapy, 32* (1), 59–73. https://doi.org/10.1016/j.ymthe.2023.11.018

Zeng, S. K., Zhang, C. H., & Jiang, Z. H. (2002). Study on the comparison of the food nutrient contents between the muscle and head of *Muraenesox Cinereus. Marine Sciences, 5*, 13–15.

Zhang, D., Guo, X., Wang, Q., Zhao, L. Y., Sun, Q. C., Duan, X. L., Cao, Y. P., & Sun, H. (2022). Investigation on lipid profile of peanut oil and changes during roasting by lipidomic approach. *LWT, 154*, Article 112594. https://doi.org/10.1016/j.lwt.2021.112594

Zhang, J., Tao, N. P., Zhao, Y. L., Wang, X. C., & Wang, M. F. (2019). Comparison of the fatty acid and triglyceride profiles of big eye tuna (*Thunnus obesus*), Atlantic salmon (*Salmo salar*) and bighead carp (*Aristichthysnobilis*) heads. *Molecules, 24*(21). https://doi.org/10.3390/molecules24213983. Article 21.

Zhang, Y. F., Zhang, M., Dong, L. P., Chang, J., Wang, H. X., & Shen, Q. (2022). Lipidomics screening of polyunsaturated phospholipid molecular species in crab (*Portunus trituberculatus*) muscular tissue: A nontarget approach by HILIC-MS. *European Journal of Lipid Science and Technology, 124*(3), 2100097. https://doi.org/10.1002/ejlt.202100097